

Article

NMR and MRI Obtained with High Transition Temperature DC SQUIDS

R.E. de Souza^{a,‡}, *K. Schlenga*^{b,†}, *A. Wong-Foy*^a, *R. McDermott*^b,
A. Pines^a, and *John Clarke*^b

^a*Department of Chemistry, University of California, Berkeley and Materials Sciences
Division, Lawrence Berkeley National Laboratory, Berkeley, CA 94720, USA*

^b*Department of Physics, University of California, Berkeley, and Materials Sciences
Division, Lawrence Berkeley National Laboratory, Berkeley, CA, 94720, USA*

Usando um espectrômetro baseado em um SQUID (dispositivo supercondutor de interferência quântica), de alta temperatura de transição, polarizado continuamente, medimos sinais de ressonância magnética nuclear (RMN) de várias amostras a temperatura ambiente em campos magnéticos na faixa entre 0,05 mT e 2 mT. É possível observar sinais de prótons em uma amostra com 1 mL de óleo mineral em 2 mT com apenas uma aquisição. A sensibilidade do sistema também permite a detecção de RMN de prótons em um campo magnético tão baixo quanto 0,059 mT, o qual é comparável ao campo da Terra. Estes resultados tornam possíveis vários outros experimentos em imagens por ressonância magnética nuclear. Apresentamos uma imagem em duas dimensões obtida a temperatura ambiente em um campo magnético de 2 mT a partir de um padrão com uma estrutura interna preenchida com óleo mineral.

We have measured nuclear magnetic resonance (NMR) signals from several samples at room temperature in magnetic fields ranging from about 0.05 mT to 2 mT using a spectrometer based on a high- T_c dc SQUID (high transition temperature dc Superconducting QUantum Interference Device). We are able to observe proton signals from 1 mL of mineral oil in 2 mT in a single transient. The sensitivity of this system has also allowed the detection of proton NMR at magnetic fields as low as 0.059 mT, which is comparable to the Earth's field. Such results make possible a number of new experiments in magnetic resonance imaging (MRI). We present a two-dimensional image of a phantom filled with mineral oil obtained in a field of 2 mT.

Keywords: *NMR, MRI, SQUID detected NMR*

Introduction

In a typical NMR experiment, the signal is proportional to the product of nuclear magnetization¹ and the Larmor frequency. Since both magnetization and precession frequency scale with magnetic field strength, the NMR signal is greatly enhanced as magnetic field is increased. However, for systems with short-range order, such as amorphous and polycrystalline materials, high-field NMR spectra are broad and hard to resolve. In such systems, the random molecular orientation with respect to the applied magnetic field causes different local Larmor frequencies at each molecular site. Therefore, the spectra display a characteristic "powder pattern"². Several techniques have been developed to narrow these spectra and facilitate the ac-

quisition of structural information³. An alternate approach is to detect NMR signals at magnetic fields that are low compared to local fields, so that all equivalent sites have the same resonance frequency; thus, the spectra are considerably simplified. However, for conventional NMR detectors, the signal-to-noise (S/N) ratio is markedly reduced in low field⁴, making data acquisition extremely time consuming. SQUID-detected NMR offers an alternative solution to this problem. While conventional pickup coils measure the time derivative of a magnetic flux⁵, SQUIDS measure the magnetic flux directly⁶. This leads to a much higher S/N ratio at low frequencies.

Over the last decade, low transition temperature (low- T_c) SQUIDS have been employed in numerous experiments

‡Permanent address: Departamento de Física, Universidade Federal de Pernambuco, Av. Prof. Luiz de B. Freire, s/n, 50670-901 Cidade Universitária, Recife - PE, Brazil

†Present address: BRUKER Analytische Messtechnik, Wikingenstr. 13, 76189 Karlsruhe, Germany

to detect NMR and nuclear quadrupole resonance (NQR) signals⁷⁻¹⁴. Even for magnetic resonance imaging (MRI), where static and/or time-dependent magnetic field gradients are applied, low- T_c SQUIDs have proven to be a sensitive and stable sensor¹⁵⁻¹⁶. However, low- T_c SQUIDs must be operated at liquid helium temperatures. At this low temperature, the number of samples having sufficiently short spin-lattice relaxation times to allow for signal averaging in pulsed experiments is limited. Low- T_c SQUIDs are inconvenient for NMR investigations of biological samples at room temperature because of the relatively complicated cryogenics involved. Nevertheless, low- T_c SQUID NMR experiments were reported by Seton *et al.*^{12,16} and Kumar *et al.*^{13,14}. Later Kumar *et al.*¹⁷ used a high- T_c SQUID with simpler cryogenics for the detection of NMR signals.

The aim of this article is to present a new high- T_c dc SQUID spectrometer that is able to detect NMR signals from samples at room temperature in magnetic fields as low as 0.059 mT. The feasibility of NMR detection in these low fields is demonstrated with spectral data of ^1H , ^{19}F , and laser-polarized ^{129}Xe nuclei. In addition, we have implemented a system of magnetic field gradient coils to perform MRI under low-field conditions. Two-dimensional proton magnetic resonance images of filled phantoms have been obtained using this apparatus.

Experimental Configuration

Our spectrometer is based on a high- T_c dc SQUID operating in a flux-locked loop. The sensor is a multilayer multiloop integrated magnetometer¹⁸. In the relevant frequency range the system flux noise is $25 \mu\Phi_0/\text{Hz}^{1/2}$, where $\Phi_0 = h/2e$ is the flux quantum. Taking into account the effective area of 1.8 mm^2 , we find a magnetic field noise of $30 \text{ fT}/\text{Hz}^{1/2}$. The magnetometer is operated without a tuned input circuit; this allows for broadband detection from DC to 1.1 MHz, which is a desirable feature for multiple resonance spectroscopy. Figure 1 shows a schematic layout of the spectrometer. The voltage across the SQUID is amplified by a low-noise pre-amplifier at room temperature. After further amplification, the signal is integrated and fed back via a resistor into a single-turn coil inductively coupled to the SQUID. The voltage across the feedback resistor is further amplified and filtered (Rockland model 442) and then fed into a spectrum analyzer (Hewlett Packard-model 3561A) and a data acquisition system (Tecmag-ARIES and Macintosh-IIci). The control unit produces audio-frequency drive pulses and performs data digitization and storage. Because high power audio-frequency pulses inevitably couple excessive flux into the SQUID, driving the integrator into saturation, a reset signal is forwarded to the SQUID electronics to short the integrator during excitation pulses. The pulse sequence generated

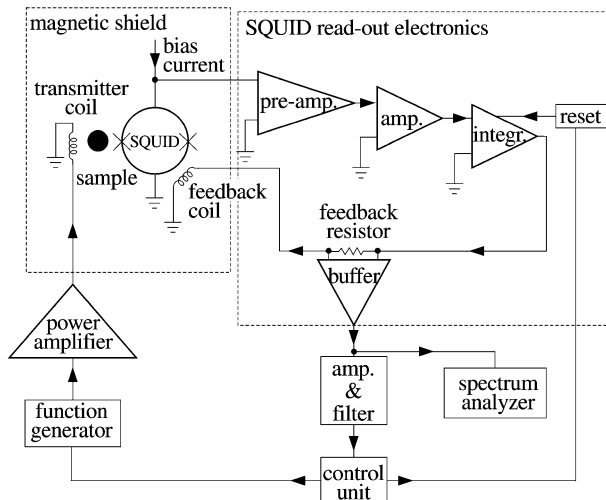


Figure 1. Schematic layout of the spectrometer. For simplicity, the cryogenic system and some of the coils are omitted.

by the Tecmag system is used to gate a function generator (Hewlett Packard 3314A) in order to produce the audio-frequency excitations. These pulses are applied to the transmitter coils after amplification by a power amplifier (Krohn-Hite-model 3322 filter).

Figure 2 shows a simplified drawing of the dewar and coil system. The SQUID magnetometer is operated in vacuum and separated from the sample by a sapphire window; the SQUID-to-sample separation is less than 1 mm. A 0.1 m long sapphire rod thermally anchored to the liquid nitrogen reservoir provides efficient cooling. The dewar is similar to that described in detail in elsewhere¹⁹. A pair of Helmholtz coils, each with a diameter of 0.12 m and 1,300 turns, produces the static magnetic field \mathbf{B}_0 . The calculated field homogeneity at the center of the coils is better than 0.07% and 0.7% correspond, respectively, to over a cubic volume of 1 cm^3 and 8 cm^3 . A three-layer mu-metal shield enclosing the dewar and coil system attenuates external fields by a factor of 1,430 at zero frequency. All experiments are carried out in an electromagnetically shielded room.

For our pulsed NMR experiments, the excitation field \mathbf{B}_1 is produced by a Helmholtz pair oriented perpendicular to the \mathbf{B}_0 direction. Each excitation coil has a diameter of 8.6 cm and contains 20 turns; the coils are tuned to the Larmor frequency of the sample. The calculated field homogeneity at the center of these coils is better than 0.12% and 1.2% correspond, respectively, to over a cubic volume of 1 cm^3 and 8 cm^3 . For the purposes of imaging we used a Maxwell pair, oriented parallel to the static field, to produce a magnetic field gradient \mathbf{G} . Each gradient coil has a diameter of 0.12 m and contains 50 turns. The linearity of the field gradient is better than 0.3% and 1.0% correspond, respectively, to over a cubic volume of 1 cm^3 and 8 cm^3 at the center of the coils. All three pairs of coils were

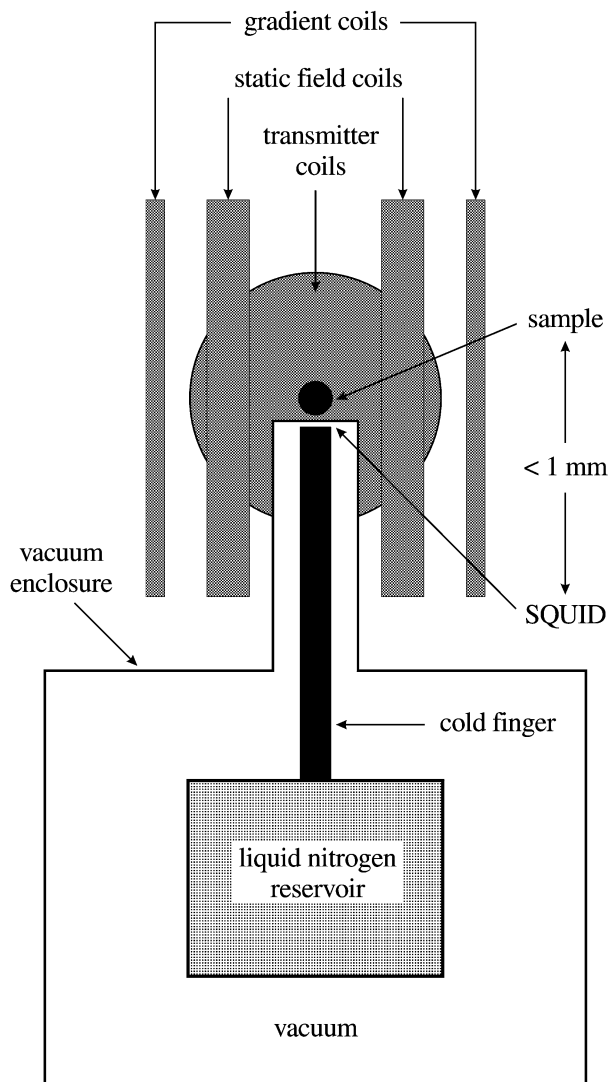


Figure 2. Liquid nitrogen dewar, SQUID, and coils.

wound from insulated copper wire and mounted on a common frame made from G-10 fiberglass and plexiglass. In order to avoid acoustic resonances in the coils, this frame was designed to be extremely rigid.

Precessing magnetization of the sample is induced by magnetic field audio-frequency pulses from the transmitter coils. We have employed Hahn spin echo²⁰ sequences for most of the spectroscopic experiments at various field values. We typically used a $\pi/2$ pulse with a field amplitude of $60 \mu\text{T}$ and a length of $200 \mu\text{s}$, followed a few milliseconds later by a π pulse with the same field amplitude. In order to avoid pickup of ringing produced in the coils by the mismatch between the coils and the signal generator, the π pulse is followed by a $100 \mu\text{s}$ delay before the SQUID feedback loop is switched on. Data acquisition begins $100 \mu\text{s}$ later. To allow the spins to relax completely the repetition rate is low, approximately 2.5 Hz.

For our NMR imaging experiments, we have employed pulse sequences with Ernst tipping angles²¹ in order to minimize acquisition time. Here we applied pulses with a field amplitude of $60 \mu\text{T}$, a length of $120 \mu\text{s}$, and a repetition rate of 25 Hz. A static magnetic field gradient of 2 mT/m is applied during the entire acquisition. For two-dimensional imaging experiments, our sample was rotated in angular steps of 15° ; for each angle we performed 30,000 averages.

Results and Discussion

Our first experiments were performed on samples with either a high density of nuclear spins or with hyperpolarized ^{129}Xe . For our ^1H samples we chose mineral oil because of its relatively short spin-lattice relaxation time T_1 and its relatively long spin-spin relaxation time T_2 . This allows us to exploit the advantage of pulsed NMR experiments and to improve the S/N ratio by signal averaging. In addition, we have measured ^1H signals from human tissue. For studies of ^{19}F nuclei we used deuterated trifluoroacetic acid, which has a T_1 value comparable to T_1 in ^1H samples. The samples of ^{129}Xe were polarized far above the equilibrium value by means of spin-exchange collisions with optically pumped rubidium, as described elsewhere^{11,22}.

A. Spectroscopic experiments

Most of our experiments were performed in magnetic fields between 1 mT and 2 mT; depending on the nuclei, the Larmor frequencies were between 10 kHz and 90 kHz. In a magnetic field of 2.03 mT we can detect the proton spin echo signal at 86.67 kHz without signal averaging. The corresponding spectrum after Fourier transformation is shown in Fig. 3(a). Given the extremely weak equilibrium polarization of ^1H nuclear spins (7×10^{-9}) at this field and room temperature, the resulting spectrum demonstrates the high sensitivity of the SQUID detection scheme. We have also performed experiments on hyperpolarized ^{129}Xe which had a pumped polarization of about 2×10^{-2} , an enhancement of seven orders of magnitude over the equilibrium polarization at room temperature. We have measured the free induction decay (FID) of ^{129}Xe with the multiloop magnetometer after a single $\pi/2$ pulse. The sample tube was 1.4 cm long and had an inner diameter of 0.5 cm. Figure 3(b) shows the Fourier transform of the ^{129}Xe FID; the S/N ratio is approximately 100. The extremely high S/N ratio attained in this experiment indicates that laser-polarized ^{129}Xe has great potential for use in SQUID MRI²³ as an agent to study voids in materials and in living systems.

In order to improve on the S/N ratio of our first experiments with protons, we averaged 1,000 times under the same conditions. The averaged spectrum of the proton spin echo is shown in Fig. 4(a). In this experiment we obtained

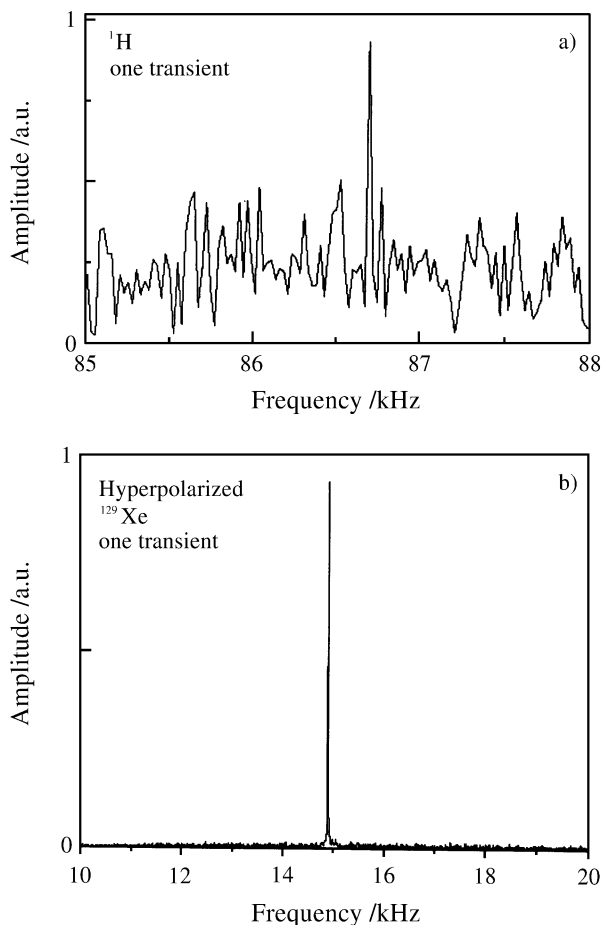


Figure 3. Single transient measurements: (a) proton NMR signal from mineral oil in a magnetic field of 2.03 mT; (b) NMR signal from hyperpolarized ^{129}Xe gas in a magnetic field of 1.27 mT.

a S/N ratio of approximately 44 with an averaging time of 10 min. Signal averaging further allowed us to resolve the proton spin echo produced by 1 mL of mineral oil in a field of 0.059 mT, which is comparable to the Earth's magnetic field. Even though the equilibrium spin population of protons in mineral oil at room temperature, $\hbar\omega_0 / k_B T$, is only 2×10^{-10} , we observe a clear peak at 2.5 kHz after 2,000 averages²⁴. We might note that while Packard *et al.*²⁵ have reported NMR in the Earth's magnetic field, their experiments were carried out with the aid of prepolarization techniques.

We have demonstrated the system's ability to measure NMR signals from nuclei other than ^1H in thermal equilibrium. We chose fluorine for its high gyromagnetic ratio and its environmental relevance. Figure 4(b) shows a spectrum obtained from ^{19}F nuclei in deuterated trifluoroacetic acid under the same conditions as in the previous experiment with protons.

In order to test our ability to perform NMR in living systems, we carried out experiments with human tissue. These experiments were performed without the lid of the

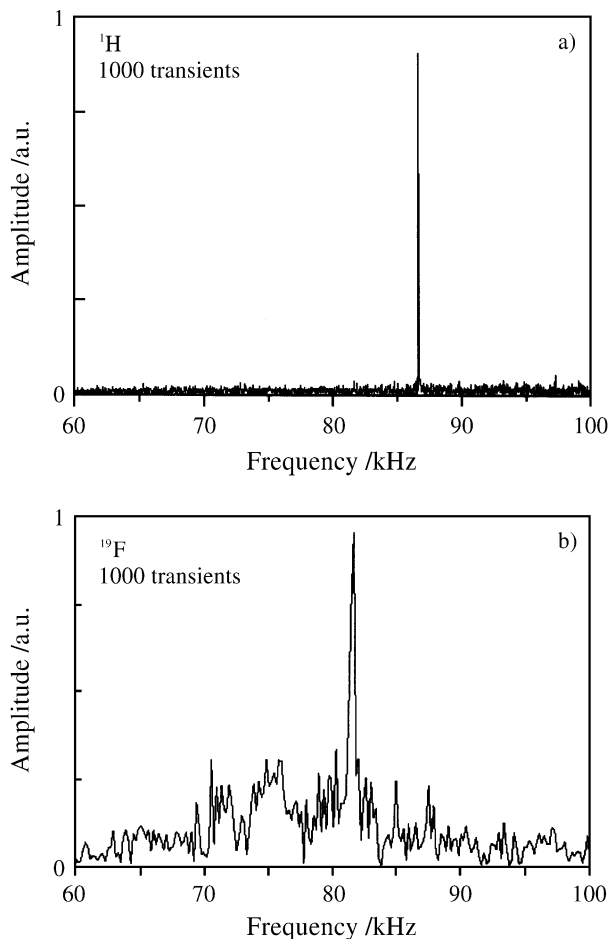


Figure 4. (a) Proton NMR signal from mineral oil in a magnetic field of 2.03 mT after 1,000 signal averages. The linewidth of approximately 70 Hz is dominated by the inhomogeneity of the static field. (b) ^{19}F -NMR signal from deuterated trifluoroacetic acid in a magnetic field of 2.03 mT after 1,000 signal averages.

mu-metal shield. We have measured the ^1H -NMR signal from the index finger of one of the authors under the same conditions as the ^1H experiments in mineral oil. The Fourier transformed spin echo of protons from the tip of an index finger is shown in Fig. 5. This important test has ruled out several expected problems, such as direct noise coupling into the SQUID from the surroundings, noise coupling to the SQUID via the finger (which might behave as an antenna), audio-frequency from the transmitter coils coupling to the SQUID via the finger, and mistuning of the transmitter coils due to the presence of the finger.

B. Imaging experiments

The high S/N ratio obtained with the multiloop magnetometer in fields of 2 mT has enabled us to obtain proton magnetic resonance images. For the purposes of imaging we must take into account the fact that the SQUID magnetometer does not enclose the sample, but rather acts as a surface coil, similar to those used in conventional

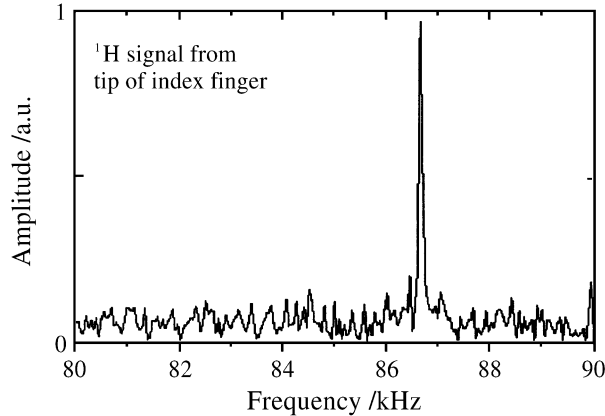


Figure 5. Proton NMR signal from the tip of an index finger in a magnetic field of 2.03 mT after 500 signal averages. The S/N ratio is approximately 7.

NMR/MRI²⁶. The intensity of the NMR signal from a given part of the sample depends on its position relative to the magnetometer. Therefore our imaging method involves both frequency encoding and position encoding of the spins in our sample²⁷. Our earliest two-dimensional imaging experiments involved a simple scheme in which the sample is placed on the top of the SQUID magnetometer and sequentially rotated in a magnetic field gradient applied parallel to the plane of the magnetometer. Hence, on resonance and with the gradient \mathbf{G} along the direction of the static magnetic field \mathbf{B}_0 , the signal at a given angular position α is given by:

$$\text{signal}(k, \alpha) = \iiint \phi(x, y, z) \cdot \rho(x, y, z) e^{2\pi i [(k \cos \alpha)x + (k \sin \alpha)z]} dx dy dz$$

where $\phi(x, y, z)$ describes the contribution of an ensemble of dipoles located at the coordinates (x, y, z) to the total magnetic flux through the magnetometer²⁷, $\rho(x, y, z)$ is the spin density at (x, y, z) , and $k = \gamma G t / 2\pi$, where γ is the gyromagnetic ratio; the center of the magnetometer defines the origin in space $(0, 0, 0)$, and the xz plane is taken to coincide with the plane of the magnetometer. Therefore the function $\text{signal}(k, \alpha)$ is intrinsically defined in a polar raster.

The linewidth in a given experiment, along with the desired spatial resolution, defines the minimum value for the magnetic field gradient necessary to obtain magnetic resonance images. From linewidth measurements on the spectrum shown in Fig. 4(a) we calculate a minimum field gradient of 0.25 mT/m in order to achieve a spatial resolution of approximately 0.35 cm. The maximum magnetic field gradient suitable for MRI experiments is mainly set by the S/N ratio attainable. In our MRI experiments we used a static magnetic field gradient of about 2 mT/m.

Using the filtering back-projection reconstruction method^{28,29} we calculate the imaging function, given by

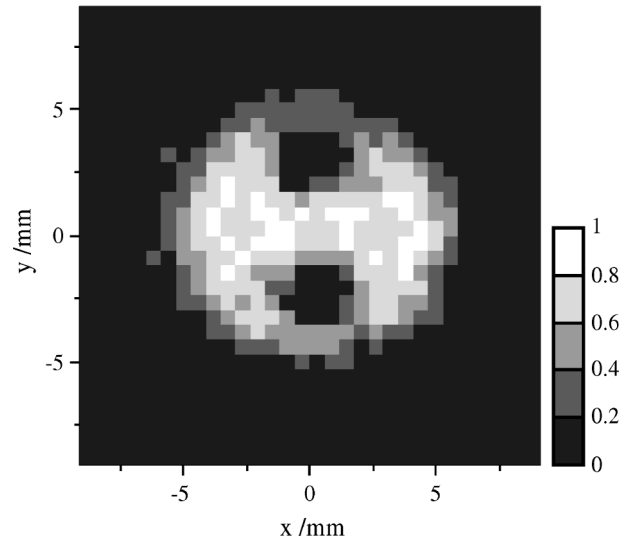


Figure 6. Raw two-dimensional NMR image of a phantom filled with mineral oil. The image results from 24 angular steps of 15° each with 30,000 averages collected at 2.03 mT.

$$\text{Image}(x, z) = \int \rho(x, y, z) dy$$

This function represents the spin density distribution of the sample projected along the y direction (the vertical direction in our experiments). For objects with axial symmetry, the function $\phi(x, y, z)$ can be considered constant. For objects with quasi-axial symmetry, $\phi(x, y, z)$ can be taken to be nearly constant for points in the sample whose distance from the center of magnetometer is roughly comparable to the magnetometer radius. Therefore, for our magnetometer dimensions, the linear sample size should be about 0.4 cm.

We measured $\text{signal}(k, \alpha)$ from a sample consisting of 0.6 mL of mineral oil in a cylindrical container of 0.7 cm diameter and 2 cm height. Two glass rods were placed inside the container, aligned with the container axis and positioned roughly along the container diameter. In Fig. 6 we show a gray scale plot of the function $\text{Image}(x, z)$ for the phantom described above. From the measured linewidth of 70 Hz without an applied magnetic field gradient, we estimate the spatial resolution to be about 800 μm . We might note that it is possible to acquire the signal function in Cartesian coordinates by using pulsed magnetic field gradients^{30,31}. With this end in mind, a new system of coils, gradient power amplifiers, and gradient controllers, is currently being developed.

Conclusions

We have developed a novel system for SQUID-detected NMR and MRI studies of samples at room temperature and in magnetic fields ranging from 59 μT to 2000 μT . This system can accommodate samples of 1 cm scale and larger, thereby permitting spectroscopy of biological samples. We

have observed NMR signals from protons, fluorine, and hyperpolarized ^{129}Xe . In particular, proton NMR signals have been measured from samples in thermal equilibrium at room temperature and in a magnetic field comparable to that of the Earth. We have acquired low-field proton NMR data from the tip of a finger, suggesting that we could perform MRI on living tissue. We have also obtained two-dimensional MRI from phantoms filled with mineral oil. We plan to extend our NMR experiments to other nuclei, as well as to implement NQR to study systems with quadrupole nuclei. Efforts are underway to incorporate pulsed gradients into our two-dimensional imaging scheme. Finally, we note that although our high- T_c dc SQUID-based detector has produced impressive proton NMR signals at 2 mT, one could further improve the S/N ratio, for spectroscopic purposes, by means of prepolarization techniques or dynamic nuclear polarization (DNP), depending on the system in study.

With regard to the ^{129}Xe studies, a self-contained gas flow system is currently under construction that will permit continuous optical pumping. The high sensitivity of the SQUID-based detector at low magnetic fields and the high magnetization of hyperpolarized ^{129}Xe can be combined to perform high resolution MRI of voids, for instance, in granular and porous media. It should also be possible to perform low-field NMR imaging of hyperpolarized ^{129}Xe dissolved in solution, which would be attractive for future *in vivo* studies.

Acknowledgments

We thank D.M. TonThat for helpful advice during the early phase of this project. The multiloop magnetometer was fabricated in 1994 by Frank Ludwig. This work was supported by the Director, Office of Energy Research, Office of Basic Energy Sciences, Materials Sciences Division, of the U.S. Department of Energy under Contract No. DE-AC03-76SF00098, the Deutsche Forschungsgemeinschaft, and the Brazilian Agency for Research CNPq.

References

1. Abragam, A. *The Principles of Nuclear Magnetism*; Oxford University Press; Oxford, 1961.
2. Harris, R.K. *Nuclear Magnetic Resonance Spectroscopy*; Longman Scientific & Technical; Harlow, 1986.
3. Mehring, M. *Principles of High Resolution NMR in Solids*; Springer-Verlag, Berlin, 1983.
4. do Nascimento, G.C.; Engelsberg; de Souza, R.E. *Measur. Sci. Tech.* **1992**, *3*, 370.
5. Hout, D.I.; Richards, R.E. *J. Magn. Reson.* **1976**, *24*, 71.
6. Clarke, J. *SQUID Sensors: Fundamentals, Fabrication and Applications*, Kluwer Academic, Dordrecht, 1996.
7. Hilbert, C.; Clarke, J.; Sleator, T.; Hahn, E. *Appl. Phys. Lett.* **1985**, *47*, 637.
8. Fan, N.Q.; Clarke, J. *Rev. Sci. Instrum.* **1991**, *62*, 1453.
9. Black, B.; Majer, G.; Pines, A. *Chem. Phys. Lett.* **1993**, *201*, 550.
10. TonThat, D.M.; Clarke, J. *Rev. Sci. Instrum.* **1996**, *67*, 2890.
11. TonThat, D.M.; Ziegeweid, M.; Song, Y.-Q.; Munson, E.J.; Appelt, S.; Pines, A.; Clarke, J. *Chem. Phys. Lett.* **1997**, *272*, 245.
12. Seton, H.C.; Bussell, D.M.; Hutchison, J.M.S.; Nicholson, I.; Lurie, D.J. *Phys. Med. Biol.* **1992**, *37*, 2133.
13. Kumar, S.; Thorson, B.D.; Avrin, W.F. *J. Magn. Reson. Series B*, **1995**, *107*, 252.
14. Kumar, S.; Avrin, W.F.; Whitecotton, B.R. *IEEE Trans. Magnetics*, **1996**, *32*, 5261.
15. Augustine, M.P.; Wong-Foy, A.; Yarger, J.L.; Tomaselli, M.; Pines, A.; TonThat, D.M.; Clarke, J. *Appl. Phys. Lett.* **1998**, *72*, 1908.
16. Seton, H.C.; Hutchison, J.M.S.; Bussell, D.M. *IEEE Trans. on Applied Superconductivity*, **1997**, *7*, 3213.
17. Kumar, S.; Matthews, R.; Haupt, S.G.; Lathrop, D.K.; Takigawa, M.; Rozen, J.R.; Brown, S.L.; Koch, R.H. *Appl. Phys. Lett.* **1997**, *70*, 1037.
18. Ludwig, F.; Dantsker, E.; Kleiner, R.; Koelle, D.; Clarke, J.; Knappe, S.; Drung, D.; Koch, H.; Alford, N. McN.; Button, T.W. *Appl. Phys. Lett.* **1995**, *66*, 1418.
19. Lee, T.S.; Dantsker, E.; Clarke, J. *Rev. Sci. Instrum.* **1996**, *67*, 4208.
20. Hahn, E.L. *Phys. Rev.* **1950**, *80*, 580.
21. Ernst, R.R.; Anderson, W.A. *Rev. Sci. Instrum.* **1966**, *37*, 93.
22. T.G. Walker, T.G.; Happer, W. *Rev. Mod. Phys.* **1997**, *60*, 629.
23. Tseng, C.H.; Wong, G.P.; Pomeroy, V.R.; Mair, R.W.; Hinton, D.P.; Hoffmann, D.; Stoner, R.E.; Hersman, F.W.; Cory, D.G.; Walsworth, R.L. *Phys. Rev. Lett.* **1998**, *81*, 3785.
24. Schlenga, K.; de Souza, R.E.; Wong-Foy, A.; Pines, A.; Clarke, J. *Appl. Phys. Lett.* submitted for publication.
25. Packard, M.; Varian, R. *Phys. Rev.* **1954**, *93*, 941.
26. Harten, M.D.; *Med. Phys.* **1987**, *14*, 616.
27. Schlenga, K.; de Souza, R.E.; Wong-Foy, A.; Pines, A.; Clarke, J. *IEEE Trans. on Applied Superconductivity*, **1999**, in press
28. Mansfield, P.; Morris, P.G. *NMR Imaging in Bio-Medicine*, Academic Press, New York, 1982.
29. Jain, A.K. *Fundamentals of Digital Image Processing*, Prentice-Hall Inc, Englewood Cliffs, 1989.
30. Bottomley, P.A. *J. Phys. E: Sci. Inst.* **1981**, *14*, 1081.
31. Callaghan, P.T. *Principles of Nuclear Magnetic Resonance Microscopy*, Oxford University Press, Oxford, 1991.